

# Large photoresponsivity in semiconducting BaSi<sub>2</sub> epitaxial films grown on Si(0 0 1) substrates by molecular beam epitaxy

著者別名	都甲 薫, 末益 崇
journal or publication title	Journal of crystal growth
volume	378
page range	198-200
year	2013-09
権利	(C) 2013 Elsevier B.V. NOTICE: this is the author ' s version of a work that was accepted for publication in Journal of crystal growth. Changes resulting from the publishing process, such as peer review, editing, corrections, structural formatting, and other quality control mechanisms may not be reflected in this document. Changes may have been made to this work since it was submitted for publication. A definitive version was subsequently published in Journal of crystal growth, 378, 2013 <a href="http://dx.doi.org/10.1016/j.jcrysgro.2012.12.052">http://dx.doi.org/10.1016/j.jcrysgro.2012.12.052</a>
URL	<a href="http://hdl.handle.net/2241/119788">http://hdl.handle.net/2241/119788</a>

doi: 10.1016/j.jcrysgro.2012.12.052

1 **Large photoresponsivity in semiconducting BaSi<sub>2</sub> epitaxial films grown**  
2 **on Si(001) substrates by molecular beam epitaxy**

3 S. Koike<sup>a</sup>, K. Toh<sup>a</sup>, M. Baba<sup>a</sup>, K. Toko<sup>a</sup>, K. O. Hara<sup>b</sup>, N. Usami<sup>b,c</sup>, N. Saito<sup>d</sup>,

4 N. Yoshizawa<sup>d</sup>, T. Suemasu<sup>a,c</sup>

5 <sup>a</sup>*Institute of Applied Physics, University of Tsukuba, Tsukuba, Ibaraki 305-8573, Japan*

6 <sup>b</sup>*Institute for Materials Research, Tohoku University, Sendai, Miyagi 980-8577,*

7 *Japan*

8 <sup>c</sup>*Japan Science and Technology Agency, CREST, Chiyoda, Tokyo 102-0075, Japan*

9 <sup>d</sup>*National Institute of Advanced Industrial Science and Technology, Tsukuba,*

10 *Ibaraki 305-8568, Japan*

11

12 **Corresponding author:** T. Suemasu

13 Institute of Applied Physics, University of Tsukuba, Tsukuba, Ibaraki 305-8573,

14 Japan

15 TEL/FAX: +81-29-853-5111, Email: [suemasu@bk.tsukuba.ac.jp](mailto:suemasu@bk.tsukuba.ac.jp)

16

17 Approximately 900- and 400-nm-thick BaSi<sub>2</sub> epitaxial films were grown on Si(111)  
18 and Si(001) substrates, respectively, by molecular beam epitaxy, and their  
19 photoresponse properties were compared at room temperature. When the bias  
20 voltage  $V_{\text{bias}}$  applied between the 1.5-mm-spacing stripe-shaped electrodes on the  
21 BaSi<sub>2</sub> surfaces increased, photocurrents were clearly observed for photon energies  
22 greater than the band gap for both samples. However, the photoresponsivity for  
23 BaSi<sub>2</sub> on Si(001) was more than 8 times larger than that for BaSi<sub>2</sub> on Si(111);  
24 reaching approximately 50 and 5 mA/W at 1.6 eV, respectively, when  $V_{\text{bias}}$  was 1.0  
25 V. This is attributed to the difference in the grain size of BaSi<sub>2</sub> films confirmed by  
26 plan-view transmission electron microscopy.

27

28

29 PACS: 78.40.Fy

30 **Keywords:** B1. Semiconducting silicides; B2. BaSi<sub>2</sub>; B3. Solar cell; A3. MBE; A1.

31 Large grain

32

33

## 34 1. Introduction

35 It is important for solar cell materials to have a large absorption coefficient  
36 and a suitable band gap that matches the solar spectrum to yield high conversion  
37 efficiency. Among such materials, we have focused on semiconducting  
38 orthorhombic BaSi<sub>2</sub>. The band gap of BaSi<sub>2</sub> is approximately 1.3 eV and can be  
39 increased up to 1.4 eV in Ba<sub>1-x</sub>Sr<sub>x</sub>Si<sub>2</sub> [1,2], which matches the ideal solar spectrum  
40 much better than crystalline Si. In addition, BaSi<sub>2</sub> has a very large absorption coefficient  
41  $\alpha$  of approximately  $3 \times 10^4 \text{ cm}^{-1}$  at 1.5 eV [2]. A large value of  $\alpha$  and expansion of the  
42 band gap in Ba<sub>1-x</sub>Sr<sub>x</sub>Si<sub>2</sub> were theoretically expected [3,4]. BaSi<sub>2</sub> can be grown  
43 epitaxially on a Si(111) substrate with the orientation alignment of  
44 BaSi<sub>2</sub>(100)//Si(111), with a small lattice mismatch of 1.0% for BaSi<sub>2</sub>[010]//Si[112]  
45 [5]. Therefore, lots of studies have been done on BaSi<sub>2</sub> epitaxial films grown on  
46 Si(111) by molecular beam epitaxy (MBE). Recently, we have achieved large  
47 photoresponsivity in undoped *n*-type BaSi<sub>2</sub> epitaxial layers on Si(111) and  
48 polycrystalline BaSi<sub>2</sub> layers on (111)-oriented polycrystalline Si layers on SiO<sub>2</sub>  
49 [6-8]. With respect to the lattice mismatch, we have considered that the (111) facet  
50 of a Si substrate is best for BaSi<sub>2</sub> growth, although the grain size of BaSi<sub>2</sub> is as  
51 small as approximately 0.2  $\mu\text{m}$  [9]. This is because of three epitaxial variants, due

52 to the sixfold symmetry of Si(111) [10], rotating around each other by  $120^\circ$  in the  
53 surface normal. Many grain boundaries and other defects in a film would deteriorate  
54 the optical and electrical properties. Thus, it is important to increase the grain size  
55 of BaSi<sub>2</sub> films. Note that *a*-axis oriented BaSi<sub>2</sub> was surprisingly grown on the  
56 Si(001) substrate, despite the large lattice mismatch of 0.1% for  
57 BaSi<sub>2</sub>[001]//Si[110] and 12.5% for BaSi<sub>2</sub>[010]//Si[110] [5]. Very recently, we  
58 found that the grain size of *a*-axis-oriented BaSi<sub>2</sub> epitaxial layers on Si(001) is more  
59 than 1  $\mu\text{m}$ , much larger than that on Si(111) [11]. However, we have not yet  
60 measured photoresponse properties of BaSi<sub>2</sub> epitaxial films on Si(001). In this paper,  
61 we aimed to compare the photoresponsivity of BaSi<sub>2</sub> grown on Si(001) with that on  
62 Si(001), already reported in Ref. [7].

63

## 64 **2. Experimental**

65 An ion-pumped MBE system equipped with standard Knudsen cells for Ba  
66 and Sb, and an electron-beam evaporation source for Si was used. After cleaning  
67 Czochralski n-Si(111) ( $\rho=0.015 \text{ }\Omega\cdot\text{cm}$ ) and n-Si(001) ( $\rho=0.07 \text{ }\Omega\cdot\text{cm}$ ) substrates at  
68  $850 \text{ }^\circ\text{C}$  for 30 min in ultrahigh vacuum, approximately 850- and 350-nm-thick  
69 undoped *n*-BaSi<sub>2</sub> epitaxial films were grown on Si(111) and Si(001) substrates,

70 respectively, by reactive deposition epitaxy (RDE; Ba deposition on hot Si) for  
71 BaSi<sub>2</sub> template layers, and subsequent MBE (codeposition of Ba and Si on Si) to  
72 form thick BaSi<sub>2</sub> films. Details of the growth procedure have been previously  
73 described [7,11]. Finally, approximately 50-nm-thick Sb-doped n<sup>+</sup>-BaSi<sub>2</sub> (~10<sup>20</sup>  
74 cm<sup>-3</sup>) layer was formed for ohmic contacts [12]. For photoresponse measurements,  
75 Cr and Au were evaporated on the surface to form 1.5-mm-spacing stripe-shaped  
76 electrodes. The photocurrent flowing in the lateral direction between the electrodes was  
77 evaluated by a lock-in technique using a 150 W Xenon lamp (5 mW/cm<sup>2</sup> at 470 nm)  
78 with a 25-cm focal-length single monochromator (Bunkoukeiki SM-1700A). The light  
79 intensity was calibrated by a pyroelectric sensor (MELLES GRIOT 13PEM001/J). The  
80 crystalline quality of the grown films was characterized by reflection high-energy  
81 electron diffraction (RHEED), X-ray diffraction (XRD), and transmission electron  
82 microscopy (TEM).

83

### 84 **3. Results and discussion**

85 Figure 1 show the RHEED patterns of BaSi<sub>2</sub> films after (a) RDE at 550 °C  
86 and (a') MBE at 600 °C on Si(111), and after (b) RDE at 530 °C and (b') MBE at  
87 580 °C on Si(001) substrates. The RHEED patterns were observed along the Si[11-2]

88 and Si[110], respectively. We can see clear streaky RHEED patterns for BaSi<sub>2</sub> films  
89 on Si(111), which is typical for *a*-axis-oriented BaSi<sub>2</sub> epitaxial films [13]. On the  
90 other hand, two clear sets of streaky patterns with different spacings are seen for  
91 BaSi<sub>2</sub> on Si(001), in Figs. 1(b) and 1(b'). The ratio of wide streaky spacing to  
92 narrow spacing is approximately 1.7, which is explained by the ratio of  $1/b$  to  $1/c$ .  
93 Taking into account that the electron beam was incident along the Si[110] azimuth,  
94 these two streaky patterns with different spacings indicate the existence of two epitaxial  
95 variants rotating 90° to each other in the surface normal; BaSi<sub>2</sub>(100)//Si(001) with  
96 BaSi<sub>2</sub>[010]//Si[110] and BaSi<sub>2</sub>[001]//Si[110] [11].

97         Figures 2(a) and 2(b) present the  $\theta$ - $2\theta$  XRD patterns of BaSi<sub>2</sub> films on  
98 Si(111) and Si(001) substrates, respectively. The diffraction peaks at  $2\theta = 20^\circ, 41^\circ,$   
99  $63^\circ$  correspond to BaSi<sub>2</sub>(200), (400), and (600) planes, respectively, indicating that  
100 highly *a*-axis-oriented BaSi<sub>2</sub> films were grown.

101         Figures 3(a) and 3(b) shows the plan-view bright-field (BF) TEM images of  
102 BaSi<sub>2</sub> films on (a) Si(111) and (b) Si(001) substrates. The incident electron beam was  
103 almost parallel to the BaSi<sub>2</sub>[100] zone axis, but was slightly tilted for the grain  
104 boundaries (GBs) to be seen clearly. We can easily see that the grain size of the BaSi<sub>2</sub>  
105 film on Si(111) is approximately 0.2  $\mu\text{m}$ . In contrast, the grains of more than 1  $\mu\text{m}$  in

106 diameters exist in the BaSi<sub>2</sub> film on Si(001) in Fig. 3(b). We speculate that the large  
107 grain of BaSi<sub>2</sub> on Si(001) is partly due to the reduced number of epitaxial variants from  
108 three for BaSi<sub>2</sub> on Si(111) to two for BaSi<sub>2</sub> on Si(001). However, the difference in grain  
109 size is significantly larger than expected. Thus, further studies are required to clarify the  
110 mechanism that explains this difference.

111         Figures 4(a) and 4(b) show the photoresponse spectra measured at RT under  
112 various bias voltages applied between the 1.5-mm-spacing stripe-shaped Au/Cr  
113 electrodes on the surface of BaSi<sub>2</sub> films on (a) Si(111) and (b) Si(001) substrates. In  
114 both samples, photocurrents increased sharply with increasing bias voltages  $V_{\text{bias}}$  for  
115 photon energies greater than the band gap. However, the magnitude of  
116 photoresponsivity differed significantly between them. The photoresponsivity  
117 reached 13 mA/W at 1.6 eV for BaSi<sub>2</sub> on Si(111) when  $V_{\text{bias}}$  was 2.5 V on Si(111),  
118 while it marked approximately 100 mA/W for BaSi<sub>2</sub> on Si(001). This difference is  
119 attributed to the difference in the grain size of BaSi<sub>2</sub> films. It should be noted that in  
120 the photoresponse spectra, peaks become pronounced at 1.46 eV. This is due to the  
121 non-linear property of the photocurrent caused by the intense line-shaped spectrum  
122 of the Xenon light at this photon energy. On the basis of these results, we concluded  
123 that the further improvement of photoresponsivity in BaSi<sub>2</sub> epitaxial films is



124 expected with much larger grains. In this sense, a Si(001) face is more preferable  
125 for BaSi<sub>2</sub> than a Si(111) surface.

126

#### 127 4. **Summary**

128           Approximately 900- and 400-nm-thick BaSi<sub>2</sub> epitaxial films were grown on  
129 Si(111) and Si(001) substrates, respectively, by MBE. Plan-view BF TEM images  
130 revealed that the grain size of BaSi<sub>2</sub> on Si(001) was more than 1 μm, while that on  
131 Si(111) was approximately 0.2 μm. When the bias voltage  $V_{\text{bias}}$  was 2.5 V, the  
132 photoresponsivity reached 100 mA/W for BaSi<sub>2</sub> on Si(001) at 1.6 eV. On the other  
133 hand, it was only 13 mA/W for BaSi<sub>2</sub> on Si(111).

134

135 **Reference**

- 136 [1] K. Morita, M. Kobayashi, T. Suemasu, *Jpn. J. Appl. Phys.* 45 (2006) L390.
- 137 [2] K. Toh, T. Saito, T. Suemasu, *Jpn. J. Appl. Phys.* 50 (2011) 068001.
- 138 [3] D. B. Migas, V. L. Shaposhnikov, V. E. Borisenko, *Phys. Status Solidi B* 244 (2007)
- 139 2611.
- 140 [4] Y. Imai, A. Watanabe, *Thin Solid Films* 515 (2007) 8219.
- 141 [5] R. A. Mckee, F. J. Walker, *Appl. Phys. Lett.* 63 (1993) 2818.
- 142 [6] W. Du, M. Suzuno, M. A Khan, K. Toh, M. Baba, K. Nakamura, K. Toko, N. Usami,
- 143 T. Suemasu, *Appl. Phys. Lett.* 100 (2012) 152114.
- 144 [7] Y. Matsumoto, D. Tsukada, R. Sasaki, M. Takeishi, T. Suemasu, *Appl. Phys. Express*
- 145 2 (2009) 021101.
- 146 [8] D. Tsukada, Y. Matsumoto, R. Sasaki, M. Takeishi, T. Saito, N. Usami, T. Suemasu,
- 147 *Appl. Phys. Express* 2 (2009) 051601.
- 148 [9] M. Baba, K. Toh, K. Toko, N. Saito, N. Yoshizawa, K. Jiptner, T. Sekiguchi, K.
- 149 O. Hara, N. Usami, T. Suemasu, *J. Cryst. Growth* 348 (2012) 75.
- 150 [10] Y. Inomata, T. Nakamura, T. Suemasu, F. Hasegawa, *Jpn. J. Appl. Phys.* 43
- 151 (2004) L478.
- 152 [11] K. Toh, K. O. Hara, N. Usami, N. Saito, N. Yoshizawa, K. Toko, T. Suemasu, *J.*

- 153 Cryst. Growth 345 (2012) 16.
- 154 [12] M. Kobayashi, Y. Matsumoto, Y. Ichikawa, D. Tsukada, T. Suemasu, Appl.  
155 Phys. Express 1 (2008) 051403.
- 156 [13] T. Suemasu, M. Sasase, Y. Ichikawa, M. Kobayashi, D. Tsukada, J. Cryst.  
157 Growth 310 (2008) 1250.

Fig. 1 RHEED patterns of BaSi<sub>2</sub> films after (a) RDE at 550 °C and (a') MBE at 600 °C on Si(111), and after (b) RDE at 530 °C and (b') MBE at 580 °C on Si(001) substrates, observed along Si [110] and Si[11-2], respectively. The arrows show the existence of two sets of streaky patterns with different spacings for BaSi<sub>2</sub> on Si(001).

Fig. 2  $\theta$ - $2\theta$  XRD patterns of BaSi<sub>2</sub> films on (a) Si(111) and (b) Si(001) substrates. The forbidden diffraction peaks caused by the Si substrates are indicated by asterisks.

Fig. 3 Plan-view BF TEM images of BaSi<sub>2</sub> films on (a) Si(111) and (b) Si(001) substrates. The incident electron beam was almost parallel to the BaSi<sub>2</sub>[100] zone axis, but was slightly tilted for the GBs to be seen clearly.

Fig. 4 Photoresponse spectra measured at RT under various bias voltages applied between the 1.5-mm-spacing stripe-shaped Au/Cr electrodes on the surface of BaSi<sub>2</sub> films on (a) Si(111) and (b) Si(001) substrate

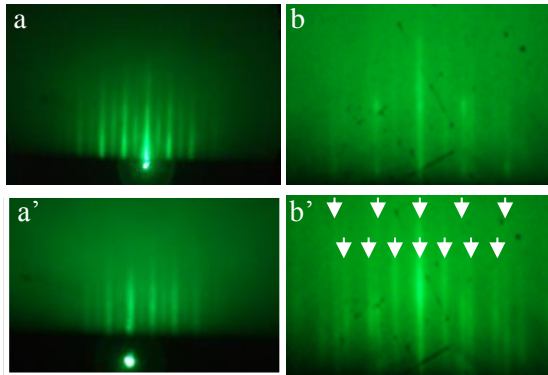


Fig. 1

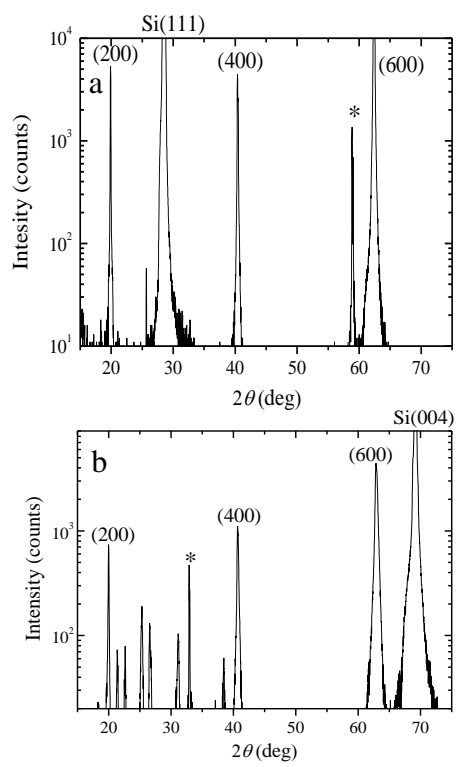


Fig. 2

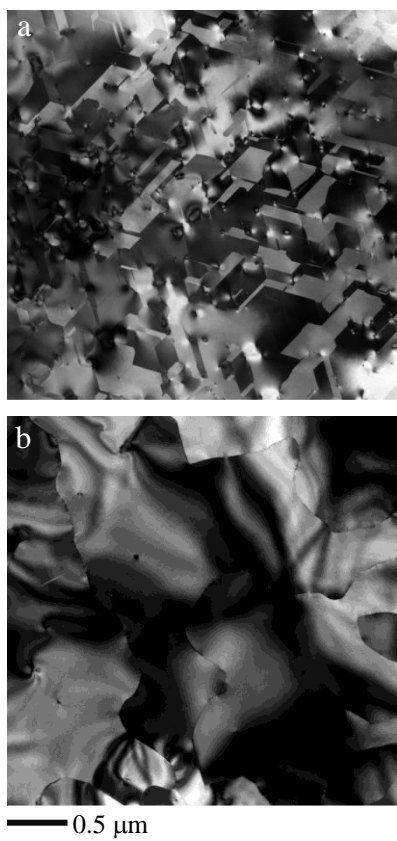


Fig. 3

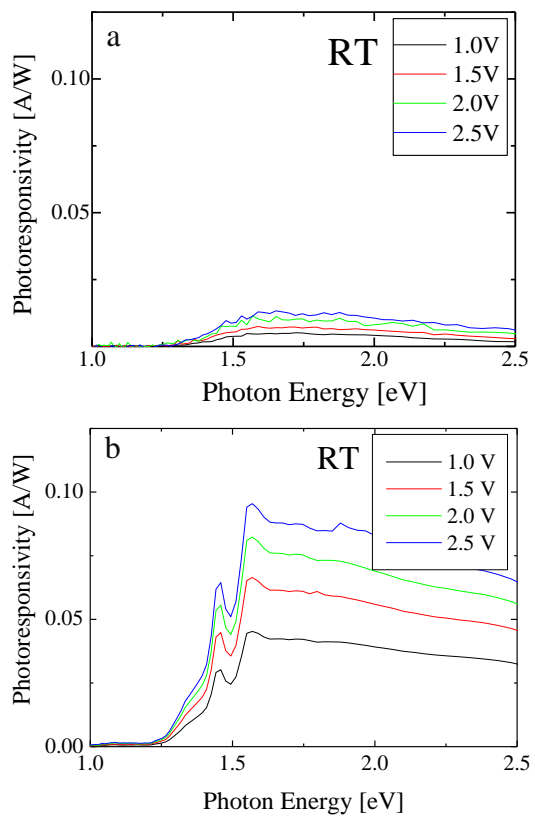


Fig. 4